

NEGATIVE GROUP VELOCITY IN A SPLIT RING RESONATOR-COUPLED MICROSTRIP LINE

G. Monti and L. Tarricone

Department Innovation Engineering
University of Salento
Via Monteroni, Lecce 73100, Italy

Abstract—The dispersive behaviour of an artificial Transmission Line is investigated demonstrating the existence of a negative group velocity region. More specifically, the propagation of amplitude modulated signals in a microstrip line coupled with Split Ring Resonators is analyzed, investigating the influence of the propagating pulse shape on the possibility to observe a negative group delay.

1. INTRODUCTION

In recent years artificial media (metamaterials) have attracted widespread interest; nowadays, their unusual properties have been investigated in a large number of papers and several applications have already been proposed.

Theoretical and experimental studies have been produced which demonstrate that an appropriate design of these media allows to achieve unusual dispersion characteristics such those corresponding to backward or superluminal propagation [1–16]; this opens up new perspectives for the so called ‘dispersion engineering’, i.e., the engineering science dealing with “the design of new classes of materials with novel and counterintuitive dispersive effects” [3].

In this paper we focus on the dispersion properties of a microstrip line coupled with Split Ring Resonator (SRR); experimental and numerical results demonstrate the existence of a negative group velocity region which has been analytically investigated by studying the propagation of amplitude modulated signals.

The paper is structured as follows: First, the superluminal propagation phenomenon is briefly introduced in Section 2, then the SRR particle is introduced in Section 3 and full-wave simulation and

Corresponding author: G. Monti (giuseppina.monti@unisalento.it).

experimental results of an SRR-coupled microstrip line are given in Section 3. Later on, Section 4 describes the analytical approach adopted for the line dispersion analysis and Section 5 illustrates the results obtained for the propagation of amplitude modulated signals. Finally some conclusions are drawn in Section 6.

2. THE NEGATIVE GROUP VELOCITY PHENOMENON

We consider an effective homogeneous medium consisting in a periodic structure made of N unit cells characterized by an effective characteristic impedance, $Z_{c,eff}$, and a per-unit cell propagation constant γ_{eff} :

$$\gamma_{eff} = \alpha_{eff} + j\beta_{eff} \quad (1)$$

With reference to a small-bandwidth propagating signal, the following velocities can be defined [23]:

- the *phase velocity* (v_p), which is the propagation velocity of a sinusoidal signal:

$$v_{p,eff} = \frac{\omega}{\beta_{eff}} \quad (2)$$

- the *group velocity* (v_g), which is the velocity by which the peak of a well-behaved wave packet travels:

$$v_{g,eff} = \left[\frac{d\beta_{eff}}{d\omega} \right]^{-1} \quad (3)$$

- the *front velocity*, which is defined as the velocity of propagation of the signal switching-on instant;

The term superluminal refers to a propagation with a group velocity negative or greater than the speed of light in vacuum (c), whilst the propagation is defined backward when the phase and group velocity are respectively negative and positive, so that the two vectors are antiparallel.

As predicted in 1968 by Veselago [1] and after the pioneering work of Smith [10] demonstrated by a large number of experimental studies, backward propagation can be observed in Double Negative (DNG) media, whilst more recently it has been demonstrated that metamaterials supporting superluminal propagation can be also designed [3–9, 11].

Particularly in [6] it has been experimentally demonstrated that superluminal propagation can be observed in a DNG medium made of alternating layers of wire arrays and SRR arrays, whilst in [7] a periodically loaded transmission line has been proposed to achieve both backward wave propagation and superluminal propagation.

In the following it will be demonstrated that similar observations can be also developed for an SRR-coupled microstrip line.

3. SPLIT RING RESONATOR-COUPLED MICROSTRIP LINE

The SRR particle is shown in Figure 1(a); it is a strongly resonant structure firstly proposed by Pendry [24] as elementary building block of a medium with negative values of the magnetic permeability.

Nowadays this particle has been studied and experimentally characterized extensively in the literature, demonstrating that an array of SRRs on a dielectric substrate exhibits negative values of the magnetic permeability around the SRR’s resonant frequency. The corresponding effective magnetic permeability is given by [6, 10]:

$$\mu_{r,eff}(\omega) = \left(1 - \frac{\omega_{pm}^2 - \omega_{om}^2}{\omega^2 + j\omega\Gamma_m - \omega_{om}^2} \right) \quad (4)$$

where Γ_m is the magnetic damping constant, whilst ω_{pm} and ω_{om} are respectively the SRR magnetic plasma and resonance frequencies. They determine the frequency range in which the SRR array behaves as an effective homogeneous medium with negative values of the

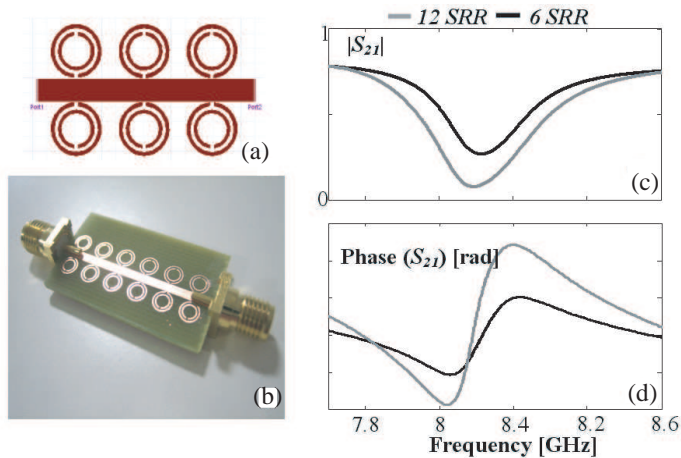


Figure 1. (a) Layout of the simulated 6 Split Ring Resonator (SRR)-coupled microstrip line. (b) Photograph of the realized 12 SRR-coupled microstrip line. (c), (d) Comparison between the full-wave simulation results achieved for the two analyzed structures: transmission coefficient amplitude (c) and phase (d).

magnetic permeability. The SRR resonant behaviour is excited by an external time-varying magnetic field perpendicular to the ring surface, inducing currents that produce a magnetic field that may either oppose or enhance the incident field, thus resulting in positive or negative effective permeability.

One of the recently proposed applications for the SRR particle consists in the possibility to generate useful stop-band or pass-band behaviours in conventional 3D or planar waveguide structures [12–23]. More specifically it has been demonstrated that a stop-band exists in a SRR-coupled microstrip line near the particle resonance frequency. In this paper we focus on the dispersion characteristics of this stop band; it will be numerically and experimentally demonstrated that it is characterized by negative values of the group velocity.

4. FULL-WAVE SIMULATION AND EXPERIMENTAL RESULTS

The analysed structure is illustrated in Figures 1(a) and 1(b): the SRR particle, which has been designed to have a resonance frequency (f_{ris}) at 8.1 GHz, has been placed near a microstrip line. The magnetic field associated to a current flow on the microstrip line is perpendicular to the SRR surface, so that it excites the resonant behaviour. This coupling mechanism generates a stop-band around the SRR resonance frequency; indeed, at f_{ris} most of the energy supplied at the input port of the microstrip line is stored in the SRRs and not delivered to the output port [24]. Furthermore, by considering the SRR equivalent circuit proposed by [25], the SRR-coupled microstrip line illustrated in Figures 1(a) and 1(b) is equivalent to a microstrip line periodically loaded with a lossy resonant circuit; consequently, according to the discussion developed in [11], we expect also negative values of the group velocity corresponding to this stop band.

Figures 1(c) and 1(d) show the full-wave simulation results achieved respectively in the case of 6 and 12 SRRs symmetrically placed near the microstrip line. More specifically simulations have been performed with the tool Momentum (Advanced Design System-Agilent) which is a full-wave planar simulator based on the Method of Moments (MoM). According to our previous observations, from Figures 1(c), (d) it can be noticed that the SRR-coupled microstrip line exhibits a stop band. It is also evident that in this band the transmission coefficient phase has a positive slope corresponding to a negative group velocity behaviour.

In order to verify these results, a 12-SRR-coupled microstrip line has been realized on a FR4 substrate (see Figure 1(b)):

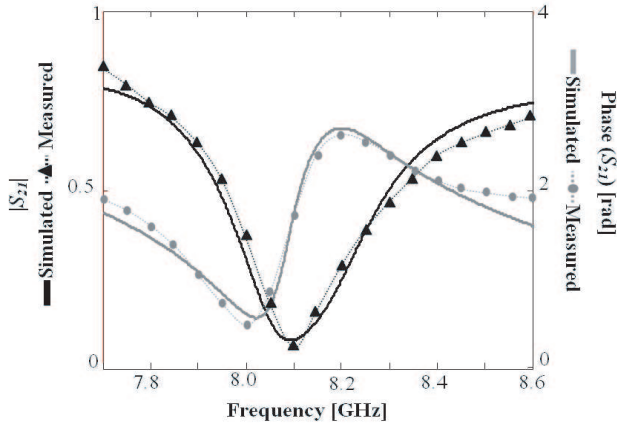


Figure 2. Comparison between the full-wave simulation results and the experimental data obtained for the transmission coefficient of the split ring resonator-coupled microstrip line illustrated in Figure 1(b).

$\epsilon_r = 3.7$, $h = 1.6$ mm, copper thickness = 0.017 mm, $(\text{tg}\delta) = 0.0023$.

Experimental results are reported in Figure 2.

5. DISPERSION ANALYSIS: METHOD FORMULATION AND IMPLEMENTATION

We consider a two-port network consisting in a periodic structure made of N unit cells characterized by an effective characteristic impedance, $Z_{c,eff}$ and a per-unit cell propagation constant γ_{eff} :

$$\gamma_{eff} = \alpha_{eff} + j\beta_{eff} \tag{5}$$

By using the network scattering parameters the following medium transfer function can be defined:

$$H(\omega) = |H(\omega)| \exp\{-j\beta_{eff}N\} = S_{21}(\omega) \tag{6}$$

Being S_{21} the network transmission coefficient.

Assuming that the signal at the input port of the network is a time harmonic electric field amplitude modulated by a slowly varying function $A(t)$:

$$\tilde{\mathbf{E}}_{in}(t, \omega_0) = E_{in}(t, \omega_0) \hat{\mathbf{u}} = A(t) \cos(\omega_0 t) \hat{\mathbf{u}} \tag{7}$$

the signal time characteristic at the output port can be calculated as

an inverse Fourier transformation (*IFT*) [11, 22]:

$$\begin{aligned} E_{out}(t) &= IFT \{ FT \{ E_{in}(t) \} H(\omega) \} \\ &= \frac{1}{\sqrt{2\pi}} 2\Re \left\{ \int_0^{+\infty} FT \{ E_{in}(t) \} S_{21}(\omega) d\omega \right\} \end{aligned} \quad (8)$$

where $E_u(\omega, \omega_0)$ is the Electric Field Fourier Transform (*FT*), and the Hermitian symmetry of $H_d(\omega)/S_{21}(\omega)$ has been used.

By discretizing the input signal and substituting the *FT/IFT* with the Discrete Fourier Transform (*DFT*)/Inverse Discrete Fourier Transform (*IDFT*), (8) can be easily solved, provided that $S_{21}(\omega)$ is known.

In this paper, by using the measured S_{21} data of Figure 2, (8) has been implemented with MATLAB and used to investigate the reshaping experienced by a signal propagating in the SRR-coupled microstrip line.

6. ANALYZED SIGNALS

According to a wide and rich discussion in the literature [26–34], in this section we use (8) with the measured data of S_{21} to study the propagation of the signal reported in (7) in the artificial TL described in Section 3.

More specifically, the shapes of the propagating signal have been fixed in order to investigate the assertions made in [31], where the NGV phenomenon has been attributed to an asymmetrical energy absorption from the propagating signal: Crisp pointed out that the attenuation experienced by a propagating pulse depends on the time derivative of its time envelope.

According to this, the analyzed signals are:

- the well known Gaussian pulse:

$$A(t) = GP(t, \sigma, \mu) = \exp \left\{ -\frac{(t - \mu)^2}{\sigma^2} \right\}, \quad (9)$$

- a signal with a not-defined amplitude peak, a raised cosine signal:

$$R(t', \rho, T_0, T) = \begin{cases} S, & |t'| \leq \frac{T_0}{2} \\ S \left\{ 1 - \sin \left[\frac{\pi}{\rho} \left(\frac{|t'|}{4T} - \frac{1}{2} \right) \right] \right\}, & |t'| \geq \frac{T_0}{2} \\ 0, & |t'| \leq \frac{T_0}{2} + 4\rho T \\ & \text{elsewhere} \end{cases} \quad (10)$$

$\rho = 0.1, T_0 = 12 \text{ ns}$

where $t' = (t - \tau)$, being τ the pulse center, while ρ , T_0 and T determine the propagating signal's time length, equal to: $(8\rho T + T_0)$ ($\rho \in [0, 1]$ is called the roll-off factor).

- a signal with an asymmetric time characteristic with respect to its amplitude peak (in the following referred as Asymmetric signal)

$$AS(t, \sigma_1, \sigma_2, \mu_1, \mu_2) = \begin{cases} [1 - F(t, \sigma_1, \mu_1)], & t \in [0, \mu_2] \\ [1 - F(\mu_2, \sigma_1, \mu_1)] F(-t, \sigma_2, -\mu_2), & t \geq \mu_2 \end{cases},$$

$$F(t, \sigma, \mu) = \exp\left\{\frac{(t - \mu)}{\sigma}\right\}$$

$$\sigma_1 = 0.5 \text{ ns}, \sigma_2 = 9 \text{ ns}, \mu_1 = 0, \mu_2 = 8\sigma_1 = 4 \text{ ns} \quad (11)$$

In this case, the signal parameters have been fixed in such a way that the pulse trailing edge portion exhibits a time derivative greater than the one corresponding to the leading portion.

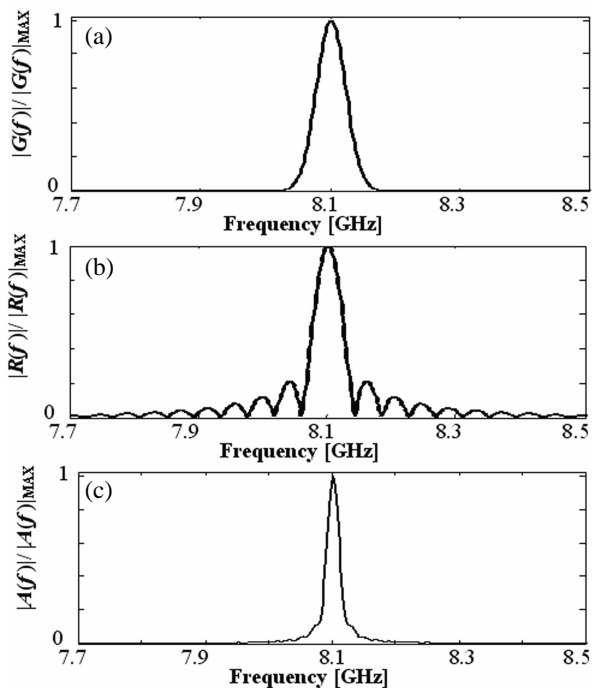


Figure 3. Spectrum amplitude of the simulated signals: (a) Small-bandwidth Gaussian pulse ($G(f)$), (b) raised cosine ($R(f)$), (c) asymmetric signal ($A(f)$).

The corresponding spectrum amplitudes are shown in Figure 3, whereas the first and second order time derivatives are given in Figure 4.

It is evident that the Gaussian pulse and the asymmetric signals are characterized by an exponential time derivative whereas the rised cosine is characterized by a sinusoidal time derivative. More important, from Figure 4 it can be noticed that the simulated signals exhibit different types of discontinuities, allowing evaluating how the ‘well-behaved’ property of the propagating pulse influences the NGV phenomenon.

In all cases the input signal carrier frequency, $f_0 = \omega_0/(2\pi)$, has been fixed equal to the SRR resonance frequency (i.e., 8.1 GHz).

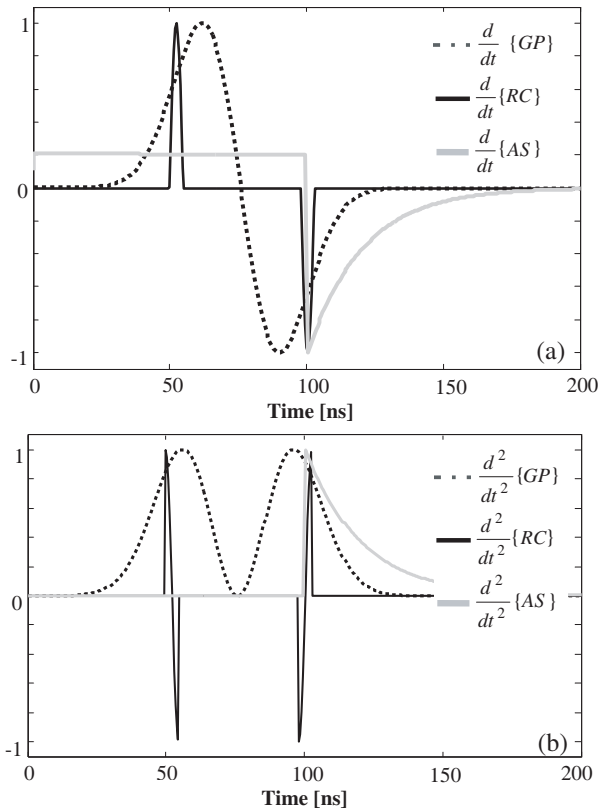


Figure 4. Normalized time derivatives of the simulated modulating signals: first (a) and second (b) order time derivatives.

6.1. Results

We start our analysis by studying the propagation of the well-behaved Gaussian pulse; three cases have been considered: a small-bandwidth Gaussian pulse ($\sigma = 20$ ns, $\mu = 100$ ns), the same signal with a jump discontinuity and a broad-band Gaussian pulse ($\sigma = 3$ ns, $\mu = 150$ ns).

Figure 5(a) shows the results achieved for the small-bandwidth Gaussian pulse (see Figure 3(a) for the corresponding spectrum amplitude); it is evident that the signal energy redistributes in such a way that the pulse amplitude peak experiences a negative group delay. In order to investigate the influence of the pulse behaviour on the superluminal propagation phenomenon, we studied the propagation of the same pulse with a discontinuity in the time envelope (see insert of Figure 5(b)); from Figure 5(b) we can see that the pulse travels at a positive group velocity experiencing a strong distorsion.

The results obtained for the broadband Gaussian pulse are reported in Figure 6: as expected the signal experiences a strong distorsion.

As for the results calculated for the raised cosine and the asymmetric signal they are given in Figure 7.

It can be noticed that the stronger distorsion is experienced by the raised cosine signal. In this case, the signal energy concentrates at the instants corresponding to the transition between the flat portion and the sinusoidal form of the pulse, which corresponds to jump discontinuities for the second-order time derivatives of the raised cosine signal time envelope.

From Figure 7(b), it is also evident that the asymmetric signal energy redistributes as in the case of the small bandwidth Gaussian pulse. However, in this case, an unperceivable negative group delay has been obtained.

In order to investigate if the distorsion experienced by the raised cosine signal is determined by the frequency dispersion of the amplitude of the S_{21} parameter, we calculated the time characteristic at the output port of the 12 SRR-coupled microstrip line by fixing in (8) $|S_{21}| = 1$ (i.e., by neglecting the system losses):

$$E_{out}(t) = \frac{2\Re}{\sqrt{2\pi}} \left\{ \int_0^{+\infty} FT\{E_{in}(t)\} \exp\{+j\text{phase}[S_{21}(\omega)]\} d\omega \right\} \quad (12)$$

Results achieved in this way are illustrated in Figure 8. By comparing Figures 7(a) and 8 it can be derived that the reshaping experienced by the raised cosine signal is mainly due to the frequency dispersion of the amplitude of the microstrip line transfer function.

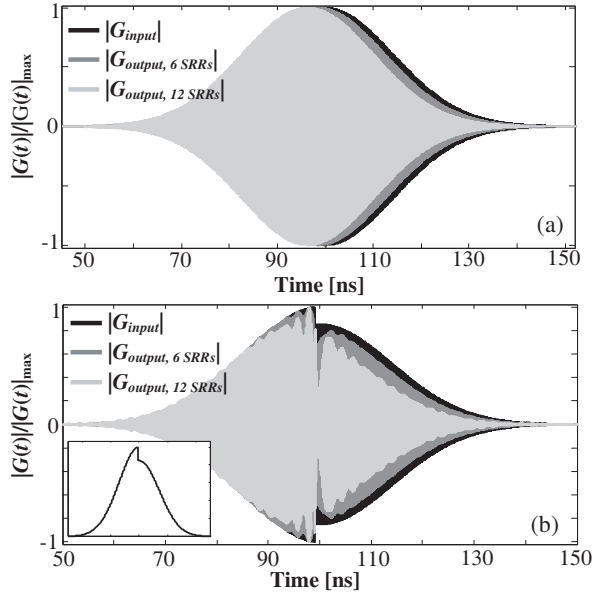


Figure 5. Normalized Gaussian pulse ($G(t)$) time characteristic calculated at the output port of the 6 and 12 split ring resonators (SRRs)-coupled microstrip line: (a) small bandwidth Gaussian pulse, (b) Gaussian pulse with a discontinuity in the time envelope (the insert shows the pulse time envelope).

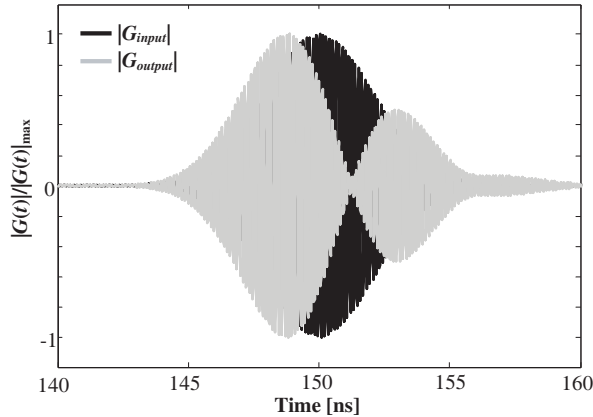


Figure 6. Normalized time characteristic calculated at the output port of the 12 SRR-coupled microstrip line in the case of broadband Gaussian pulse ($G(t)$).

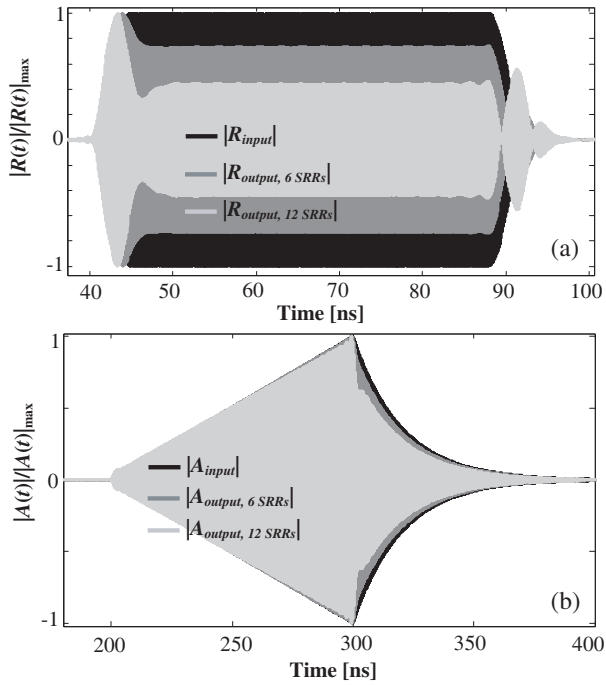


Figure 7. Time characteristics calculated at the output port of the 6 and 12 split ring resonators (SRR)-coupled microstrip line: (a) raised cosine signal ($R(t)$), (b) asymmetric signal ($A(t)$).

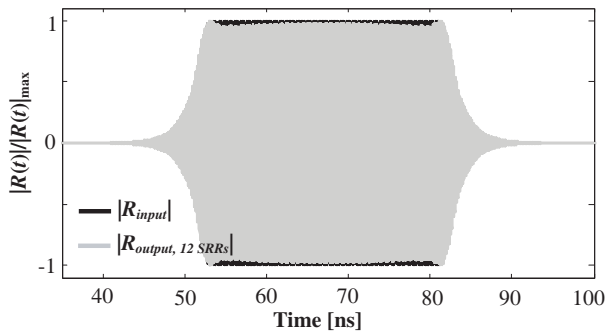


Figure 8. Results obtained for the raised cosine signal by neglecting the system losses.

7. CONCLUSION

The existence of a negative group velocity region in a microstrip line coupled with Split Ring Resonators (SRR) has been numerically and experimentally demonstrated.

By using the measured transmission coefficient, combined with an analytical approach implemented with MATLAB, the superluminal propagation mechanism has been studied by simulating the propagation of amplitude modulated signals.

In order to investigate how the signal time envelope influences the negative group velocity phenomenon, three signals with different kind of discontinuities have been considered: a gaussian pulse without discontinuity, a Gaussian pulse with a discontinuity in the time envelope and two signals with jump discontinuities in the first and second order time derivatives.

Our results demonstrate that only the well behaved Gaussian pulse, characterized by a single-lobe spectrum amplitude, experiences a negative group delay, preserving its shape during the propagation.

REFERENCES

1. Veselago, V. G., "The electrodynamics of substances with simultaneously negative values of permittivity and permeability," *Soviet Physics USPEKI*, Vol. 10, No. 4, 509–514, 1968.
2. Caloz, C. and T. Itoh, "Transmission line approach of left-handed (LH) materials and microstrip implementation of an artificial LH transmission line," *IEEE Trans. Antennas Propagat.*, Vol. 52, No. 5, 1159–1166, 2004.
3. Mojahedi, M. and G. V. Eleftheriades, *Negative Refraction Metamaterials: Fundamental Properties and Applications*, 381–411, IEEE Press-Wiley Interscience, John Wiley & Sons Inc., 2005.
4. Mojahedi, M., E. Schamiloglu, K. Agi, and K. J. Malloy, "Frequency domain detection of superluminal group velocities in a distributed bragg reflector," *IEEE Journal of Quantum Electronics*, Vol. 36, 418424, 2000.
5. Mojahedi, M., K. J. Malloy, G. V. Eleftheriades, J. Woodley, and R. Y. Chiao, "Abnormal wave propagation in passive media," *IEEE Journal of Selected Topics in Quantum Electronics*, Vol. 9, 3039, 2003.
6. Woodley, J. and M. Mojahedi, "Negative group velocity in left-handed materials," *Antennas and Propagat. Society Symp.*, Vol. 4, 643–646, 2003.

7. Siddiqui, O. F., M. Mojahedi, and G. V. Eleftheriades, "Periodically loaded transmission line with effective negative refractive index and negative group velocity," *IEEE Trans. Antennas Propagat.*, Vol. A51, No. 10, 2619–2625, 2003.
8. Mojahedi, M., E. Schamiloğlu, K. Agi, and K. J. Malloy, "Frequency domain detection of superluminal group velocities in a distributed bragg reflector," *IEEE Journal of Quantum Electronics*, Vol. 36, No. 4, 418–424, 2000.
9. Mojahedi, M. K., J. Malloy, G. V. Eleftheriades, J. Woodley, and R. Y. Chiao, "Abnormal wave propagation in passive media," *IEEE Journal of Selected Topics in Quantum Electronics*, Vol. 9, No. 1, 30–39, 2003.
10. Smith, D. R., W. J. Padilla, D. C. Vier, S. C. Nemat Nasser, and S. Schultz, "Composite medium with simultaneously negative permeability and permittivity," *Physical Review Letters*, Vol. 84, 41844187, 2000.
11. Monti, G. and L. Tarricone, "Dispersion analysis of a planar negative-group velocity transmission line," *Proc. 37th European Microwave Conf.*, 1644–1647, Munich, Germany, 2007.
12. Marqués, R., J. Mariel, F. Mesa, and F. Medina, "Left-handed simulation and transmission of EM waves in Subwavelength split-ring resonator-loaded metallic waveguide," *Physical Review Letters*, Vol. 89, No. 18, 2002.
13. Lubkowski, G., C. Damm, B. Bandlow, R. Schuhmann, M. Schübler, and T. Weiland, "Waveguide miniaturization using spiral resonator and dipole arrays," *Proc. 36th European Microwave Conf.*, 1312–1315, Manchester, UK, 2006.
14. Kondrat'ev, I. G. and A. I. Smirnov, "Comment on: 'Left-handed simulation and transmission of EM waves in subwavelength split-ring resonator-loaded metallic waveguide'," *Physical Review Letters*, Vol. 91, No. 24, 2003.
15. Yang, J., Q. Zhou, F. Zhao, X. Jiang, B. Howley, M. Wang, and R. T. Chen, "Characteristics of optical bandpass filters employing series-cascaded double-ring resonators," *Optics Communications*, Vol. 228, 91–98, 2003.
16. Falcone, F., F. Martín, J. Bonache, R. Marqués, T. Lopetegi, and M. Sorolla, "Left handed coplanar waveguide bandpass filters based on bi-layer split ring resonators," *IEEE Microw. Wirel. Compon. Lett.*, Vol. 14, No. 1, 10–12, Jan. 2004.
17. García, J. G., F. Martín, F. Falcone, J. Bonache, I. Gil, T. Lopetegi, M. A. G. Laso, M. Sorolla, and R. Marqués, "Spurious passband suppression in microstrip coupled line

- bandpass filters by means of split ring resonators,” *IEEE Microw. Wirel. Compon. Lett.*, Vol. 14, No. 9, 416–418, Sept. 2004.
18. Gil, I., J. Bonache, J. Garcia-Garcia, F. Falcone, and F. Martin, “Metamaterials in microstrip technology for filter applications,” *Antennas and Propagation Society International Symposium 2005, IEEE*, Vol. 1, 668–671, 2005.
 19. Al-Naib, I. A. I., C. Jansen, and M. Koch, “Miniaturized bandpass filter based on metamaterial resonators: A conceptual study,” *Journ. of Physics D: Applied Physics*, Vol. 41, 205002 (4), 2008.
 20. Lai, X., Q. Li, P. Y. Qin, B. Wu, and C.-H. Liang, “A novel wideband bandpass filter based on complementary split-ring resonator,” *Progress In Electromagnetics Research C*, Vol. 1, 177–184, 2008.
 21. Bahrami, H., M. Hakkak, and A. Pirhadi, “Analysis and design of highly compact bandpass waveguide filter using complementary split ring resonators (CSR),” *Progress In Electromagnetics Research*, PIER 80, 107–122, 2008.
 22. Fan, J.-W., C.-H. Liang, and X.-W. Dai, “Design of cross-coupled dual-band filter with equal-length split-ring resonators,” *Progress In Electromagnetics Research*, PIER 75, 285–293, 2007.
 23. Zhang, J., B. Cui, S. Lin, and X.-W. Sun, “Sharp-rejection low-pass filter with controllable transmission zero using complementary split ring resonators (CSR),” *Progress In Electromagnetics Research*, PIER 69, 219–226, 2007.
 24. García-García, J., F. Martín, J. D. Baena, R. Marqués, and L. Jelinek, “On the resonances and polarizabilities of split ring resonators,” *Journal of Applied Physics*, Vol. 98, No. 3, 033103-9, 2005.
 25. Baena, J. D., R. Marqués, and F. Medina, “Artificial magnetic metamaterial design by using spiral resonators,” *Physical Review B*, Vol. 69, 014402, 2004.
 26. Monti, G. and L. Tarricone, “Gaussian pulse expansion of modulated signals in a double-negative slab,” *IEEE Trans. Microwave Theory and Tech.*, Vol. 54, No. 6, 2755–2761, 2006.
 27. Brillouin, L., *Wave Propagation and Group Velocity*, Academic, New York, 1960.
 28. Pendry, J. B., A. J. Holden, D. J. Robbins, and W. J. Stewart, “Magnetism from conductors, and enhanced non-linear phenomena,” *IEEE Trans. Microwave Theory and Tech.*, Vol. 47, No. 11, 2075–84, 1999.
 29. Garrett, C. G. B. and D. E. McCumber, “Propagation of a

- gaussian light pulse through an anomalous dispersion medium,” *Physical Review A*, Vol. 1, 305313, 1970.
30. Faxvog, F. R., C. Y. Chow, T. Bieber, and J. A. Carruthers, “Measured pulse velocity greater than c in a neon absorption cell,” *Appl. Physics Letters*, Vol. 17, No. 5, 1970.
 31. Crisp, M. D., “Concept of group velocity in resonant pulse propagation,” *Physical Review A*, Vol. 5, 2104–2108, 1971.
 32. Bolda, E. L., R. Y. Chiao, and J. C. Garrison, “Two theorems for the group velocity in dispersive media,” *Physical Review A*, Vol. 48, 3890, 1993.
 33. Mitchell, M. W. and R. Y. Chiao, “Negative group delay and “fronts” in a causal system: An experiment with very low frequency bandpass amplifiers,” *Physics Letters A*, Vol. 230, 133–138, June 1997.
 34. Siddiqui, O. F., S. J. Erickson, and G. V. Eleftheriades, “Time-domain measurement of negative group delay in negative-refractive-index transmission-line metamaterials,” *IEEE Trans. Microwave Theory and Tech.*, Vol. 52, No. 5, 1449–1455, May 2004.